Novel Changes in Gene Expression following Axotomy of a Sympathetic Ganglion: A Microarray Analysis

Kristen L. Boeshore,[1] Rebecca C. Schreiber,[1] Stacey A. Vaccariello,[1] Hilary Hyatt Sachs,[1] Rafael Salazar,[1] Junghee Lee,[3] Rajiv R. Ratan,[3] Patrick Leahy,[2] Richard E. Zigmond[1]

[1] Department of Neurosciences, Case Western Reserve University School of Medicine, Cleveland, Ohio 44106

[2] Department of Comprehensive Cancer Center, Case Western Reserve University School of Medicine and University Hospitals of Cleveland, 10900 Euclid Avenue, Cleveland, Ohio 44106-4975

[3] Department of Neurology, Harvard Medical School, Boston, Massachusetts 02115

Received 1 July 2003; accepted 1 August 2003

ABSTRACT: **Neurons of the peripheral nervous system are capable of extensive regeneration following axonal injury. This regenerative response is accompanied by changes in gene expression in axotomized neurons and associated nonneuronal cells. In the sympathetic nervous system, a few of the genes affected by axonal injury have been identified; however, a broad sampling of genes that could reveal additional and unexpected changes in expression has been lacking. We have used DNA microarray technology to study changes in gene expression within 48 h of transecting the postganglionic trunks of the adult rat superior cervical ganglion (SCG). The expression of more than 200 known genes changed in the ganglion, most of these being genes not previously associated with the response to injury. In contrast, only 10 genes changed following transection of the preganglionic cervical sympathetic trunk. Real-time RT-PCR analysis verified the upregulation of a number of the axotomy-induced genes, including activating transcription factor-3 (ATF-3), arginase I (arg I), cardiac ankyrin repeat protein, galanin, osteopontin, pituitary adenylate cyclase-activating polypeptide (PACAP), parathyroid hormone-related peptide, and UDP-glucoronosyltransferase. Arg I mRNA and protein were shown to increase within neurons of the axotomized SCG. Furthermore, increases in the levels of putrescine and spermidine, a diamine and polyamine produced downstream of arg I activity, were also detected in the axotomized SCG. Our results identified many candidate genes to be studied in the context of peripheral nerve regeneration. In addition, the data suggest a potential role for putrescine and spermidine, acting downstream of arg I, in the regenerative process.** © 2004 Wiley Periodicals, Inc. J Neurobiol 59: 216–235, 2004

Keywords: **gene expression profiling; superior cervical ganglion; axotomy; regeneration; neuropeptide; microarray; nerve injury**

INTRODUCTION

Following axotomy of a peripheral neuron, the distal portion of the lesioned axon degenerates, while the proximal portion can regenerate and reinnervate denervated target tissues. Many studies have focused on molecular changes that occur distal to the site of injury in Schwann cells of the degenerating nerve tract (e.g., De Leon et al., 1991; Nagarajan, 2002). Less is known about the changes that occur proximal to this site, in particular in the cell bodies of the axotomized neurons and their associated nonneuronal cells. Historically, the earliest alteration noted in axotomized neuronal cell bodies was chromatolysis, a histological change involving the rough endoplasmic reticulum and nucleus. Matthews and Raisman (1972) proposed that chromatolysis reflected a change in the types of proteins the neurons were synthesizing. This

Correspondence to: R.E. Zigmond (rez@po.cwru.edu).

Contract grant sponsor: NIH; contract grant numbers: NS17512 and NS12651 (to R.E.Z.).

Contract grant sponsor: NIH training grant, "Cellular and Molecular Aging"; contract grant number: T32 AG00105 (to K.L.B.).

This article includes Supplementary Material available via the Internet at http://www.interscience.wiley.com/jpages/0022-3034/suppmat

DOI 10.1002/neu.10308

concept was later supported by the findings that mRNA and protein for tubulin increase after axotomy of sympathetic neurons, while those for tyrosine hydroxylase decrease (Cheah and Geffen, 1973; Koo et al., 1988). The hypothesis emerged that changes in gene expression occurring after axotomy underlie a switch in the neuron's physiological activities from neurotransmission to survival and repair. In addition to changes in the neurons themselves, axotomy of the sympathetic neurons of the superior cervical ganglion (SCG) leads to activation and proliferation of glial cells (Elfvin et al., 1987; M. Bachoo, A.K. Hall., U. Vaidyanathan, and R.E. Zigmond, unpublished observations) and to an influx, activation, and proliferation of macrophages (Schreiber et al., 1996, 2002). Changes in gene expression within nonneuronal cells of the SCG may, therefore, also contribute to survival and repair mechanisms. Although we have previously identified a small number of genes whose expression changes in the SCG in response to axotomy (for review, see Zigmond et al., 1996), a broader view of the extent of these changes has been lacking. Therefore, we have adopted a gene microarray approach to accomplish this objective.

Gene expression following decentralization (i.e., transection of the afferent input to the SCG) was also examined by microarray analysis. Decentralization results in a different set of repair needs than does axotomy. Unlike after axotomy, most SCG neurons are not injured by decentralization. However, there is degeneration of terminals of axons entering from the spinal cord and a cessation of synaptic transmission. Connections between preganglionic and postganglionic neurons need to be reformed following decentralization for recovery of normal function to occur.

Our results support the hypothesis that a switch in gene expression favoring neuronal survival and repair accompanies peripheral nerve injury. Comparison of the two types of injury revealed that axotomy has a much larger effect on gene expression within the SCG than does decentralization. Most importantly, the microarray approach identified many candidate genes that can now be studied in the context of peripheral nerve regeneration.

MATERIALS AND METHODS

Animal Surgeries

Adult male Sprague-Dawley rats (~150 g) were anesthetized by intraperitoneal injection of a mixture of ketamine, xylazine, and acepromazine. A ventral mid-cervical incision was made, and the SCGs and their afferent and efferent nerve trunks were exposed. For axotomy, the postganglionic external and internal carotid nerves (ICN and ECN) were transected at a distance of 2–3 mm from the ganglion. For decentralization of the SCG, the cervical sympathetic trunk (CST) was transected at a distance of 2–3 mm from the ganglion. In sham-operated animals, the SCG and nerve trunks were exposed, but the trunks were not cut. Following surgery, animals were allowed to recover for 6, 24, 48 h, or 5 days. Animals were then sacrificed by CO_2 inhalation and decapitation, and the SCGs were harvested and frozen on dry ice. Ganglia from intact (i.e., unoperated) control animals were also harvested. These animals differed from the sham-operated controls in that they received no incision and no anesthesia.

DNA Microarrays

Ten SCGs from five animals receiving the same surgical procedure were pooled, and total RNA was extracted using TRIzol (Invitrogen, Carlsbad, CA). First-strand cDNA synthesis was carried out by reverse transcription using 8 μg of total RNA and Superscript II (Invitrogen). Following second-strand synthesis to generate double-stranded cDNA, biotinylated cRNA probes were generated in an *in vitro* transcription reaction using the Enzo BioArray High Yield RNA Transcript Labeling Kit (Enzo Biochem, Inc., Farmingdale, NY), as per the manufacturer's protocol. Biotinylated cRNA was then fragmented and hybridized to Affymetrix RGU34A rat genomic oligonucleotide arrays (Affymetrix, Santa Clara, CA) at a concentration of 15 μg/300 μL hybridization buffer. In addition, the hybridization mix was spiked with biotinylated cRNAs for control sequences spotted onto the arrays. Approximately 200 μL of hybridization mix was added to each microarray, and hybridization was carried out for 16 h at 45°C in an Affymetrix GeneChip hybridization oven (Affymetrix). Posthybridization washes and staining procedures were carried out in an Affymetrix GeneChip Fluidics Station 4000 according to Affymetrix protocols (Affymetrix). Arrays were scanned using a Hewlett Packard Gene Array scanner. Each surgical manipulation was represented by three separate RNA preparations.

Data Analysis

Image data from the microarray scans were analyzed with Microarray Suite 5.0 (MAS 5.0; Affymetrix). MAS 5.0 was used to measure hybridization signal intensity for each gene represented on the array, to generate detection calls (a measure of whether mRNA for each gene was present, absent, or marginal in the sample applied to the array), to set up pairwise comparisons between experimental samples and controls, to calculate signal log ratios for all genes within a pairwise comparison, and to generate change calls (a measure of whether the signal log ratio for each gene within a pairwise comparison represents an increase, marginal increase, no change, marginal decrease, or decrease in expression). Because each condition was carried out in triplicate,

each of the three replicate data sets for a given condition were compared to each of the three replicate data sets for a control condition, giving rise to nine data sets for each comparison.

Comparative data resulting from analysis with MAS 5.0 was then put through a data reduction process to identify only those genes that exhibited an increase or decrease in expression following surgical manipulation (axotomy, decentralization, or sham-operation). First, signal log ratios from MAS 5.0 analysis were converted to fold change values for each gene within a comparison. Second, comparative data sets were queried to identify those genes that increased or decreased $\geq 2\times$ following a manipulation in at least six out of nine comparisons.

Subcloning Axotomy-Induced Genes

Total RNA from SCGs of axotomized rats was reverse-transcribed using oligo(dT) primers and SuperScript II (Invitrogen, Carlsbad, CA), as per the manufacturer's recommendations. Resulting cDNA was subjected to 40 rounds of PCR amplification using Platinum Taq DNA polymerase (Invitrogen) and gene specific primer pairs (see table below) for arginase I (arg I), activating transcription factor-3 (ATF-3), cardiac ankyrin repeat protein (CARP), leukemia inhibitory factor (LIF), osteopontin, parathyroid hormone-related peptide (PTHrP), ribosomal 18S protein. and UDP-glucoronosyltransferase. Primers (Qiagen, Valencia, CA) were designed to amplify fragments of approximately 200 bp. PCR products were separated by agarose gel electrophoresis and visualized with ethidium bromide staining. Bands of the expected size were extracted from the gel with a Qiagen gel extraction kit, and the eluted DNA was TA-subcloned into pDrive according to manufacturer's protocols (Qiagen). The resulting plasmids were used as positive control templates and for generation of standard curves in subsequent real-time RT-PCR time course experiments.

Real-Time RT-PCR

Using TRIzol (Invitrogen), total RNA was extracted from unoperated, sham-operated, or axotomized SCGs. RNA from the two ganglia of a single animal was used in each real-time RT-PCR reaction. Reverse-transcription of RNA into cDNA was carried out using oligo(dT) primers and SuperScript II, as per manufacturer's recommendations (Invitrogen). Real-time PCR was carried out using the iCycler system (BioRad, Hercules, CA). DNA for selected genes of interest and for the housekeeping gene (ribosomal 18S protein) were subjected to 40 rounds of amplification in the presence of SYBR green (Molecular Probes, Eugene, OR) using gene specific primers (Qiagen; designed to amplify fragments of approximately 200 bp) and Platinum Taq DNA polymerase (Invitrogen). Specificity of PCR products was determined by melt curve analysis immediately following amplification. Relative expression of genes of interest in the axotomy versus time-matched sham conditions was determined following normalization to the level of a housekeeping gene, ribosomal 18S, in each sample. Absolute levels of expression in terms of copy number were measured by comparison to standard curves for each gene of interest using 10-fold serial dilutions of plasmid cDNAs of known concentrations. Plasmid cDNAs for genes of interest were generated as described above or were obtained from colleagues (pBSK-galanin from Dr. Lee Kaplan, Harvard Medical School; pBSK-pituitary adenylate cyclase activating polypeptide (PACAP) from Dr. Victor May, University of Vermont College of Medicine). Expression of each gene of interest as well as the housekeeping gene was measured in four separate animals for each experimental condition. Sequences of the PCR primer pairs used are listed below.

Gene	Forward Primer 5′-3′	Reverse Primer 5′-3′
Arginase I (Arg I)	TACCTGCTGGGAAGGAGAA	TTCCCAAGAGTTGGGTTCAC
Activating transcription factor-3 (ATF-3)	CCCTCCTAGGGAAGATGGAG	TAGCACAACACAGGCTCAG
Cardiac ankyrin repeat protein (CARP)	TGCACTGGAGAACAAACTGC	CGCCAAGTGTCCTTCTAAGC
Galanin	GATGCCAACAAAGGGAAGA	ATAGTGCGGACGATATTGCT
Leukemia inhibitory factor (LIF)	AAGTTGGTCGAGCTGTATCG	TTCCTTTTGGAAGGCTTCTTT
Osteopontin	GATCGATAGTGCCGAGAAGC	TGAAACTCGTGGCTCTGATG
Pituitary adenylate cyclase-activating polypeptide (PACAP)	ACTTCTACGACTGGGACCCT	ACAGCCATTTGTTTTCGGTA
Parathyroid hormone-related peptide (PTHrP)	ATGACAAGGGCAAGTCCATC	TCTCCACCTTGTTGGTTTCC
UDP-glucoronosyltransferase	AGTGCAGGGTGCTCAAGAAT	TGGAGGTTCCTTCCTTGATG
Ribosomal 18 S	CCTTCGCTATCACTGCCATT	CCATCCTTCACGTCCTTCTG

In Situ Hybridization

Eight adult male rats were sacrificed at either 6 or 48 h following axotomy or sham surgery. SCGs were removed, desheathed, and immersion fixed in 4% paraformaldehyde for 1–2 h at 4°C. SCGs from four intact rats were also collected. The ganglia were then cryoprotected in sucrose and embedded in OCT. Ten-micron frozen sections were mounted on Fisher ProbeOn Plus slides, air dried for 2–3 h, and stored at −20°C. Each slide contained SCG from two

different animals for each of three different conditions (unoperated, sham operated, and axotomy). A pDrive plasmid containing a 200-bp PCR product for arg I was linearized with Bam HI and HindIII restriction enzymes. Sense and antisense probes were generated using a DIG RNA Labeling Kit (SP6/T7) from Roche (Indianapolis, IN) according to the manufacturer's instructions. DIG RNA probes were diluted in hybridization buffer (50% formamide, 5× SSC, 1 mg/mL yeast tRNA, 100 μg/mL heparin, 1× Denhardt's, 0.1% Tween 20, 0.1% CHAPS, 5 m*M* EDTA, pH 8.0, and 500 μg/mL salmon sperm DNA) at a final concentration of 1 μg/mL. The probe was heated to 80°C for 5 min and cooled to 65°C. Hybridization solution was added to the sections, and they were coverslipped with Hybrislips (Grace Bio-Labs; Bend, OR). *In situ* hybridization was performed overnight at 65°C. The cover slips were then removed by soaking in 5× SSC. Nonspecific binding was removed by high stringency washes (2× SSC, 0.2× SSC) at 65°C. Tissue sections were treated with the blocking reagent from the DIG Wash and Block kit (Roche) for 1 h at room temperature and incubated overnight at 4°C with a sheep antidigoxigenin-AP, Fab fragments antibody (Roche) diluted 1:1000 in blocking buffer. Sections were washed, and the DIG-AP conjugate was detected by the addition of NBT/BCIP color substrate solution in 0.1 *M* Tris-HCl (pH 9.5), 0.1 *M* NaCl, 50 m*M* $MgCl_2$ with 0.1% Tween-20 and 5 m*M* levamisole (to block endogenous peroxidase) for 1 to 3 days.

Western Blot Analysis

Four adult male Sprague-Dawley rats were sacrificed 48 h following axotomy or sham-operation. SCGs were removed, desheathed, and homogenized in 20 m*M* Tris-HCl buffer (pH 7.5) containing 1 m*M* EDTA, 0.5% IGEPAL CA630, 1 m*M* PMSF, and a protease inhibitor cocktail (Sigma, St. Louis, MO) containing aprotinin, pepstatin A, leupeptin, bestatin, AEBSF and E-64. The homogenates were centrifuged at 15,000 × *g* for 20 min at 4°C, and the supernatants were used as tissue extracts. Normal rat liver (1 mg wet weight) was also homogenized, and a liver extract was generated. Extracts of liver (1 μg protein) and SCG (30 μg protein) were subjected to SDS-PAGE (12% gel), and the proteins were then blotted by electrotransfer onto a PVDF membrane. The membrane was blocked with 5% nonfat dry milk in PBS with 0.1% Tween-20. The membrane was treated with a rabbit polyclonal antibody to rat liver arginase I (1:10,000), followed by immunodetection with ECL Plus Western blotting detection system (Amersham, Piscataway, NJ).

Immunohistochemistry

Four adult male rats were sacrificed 48 h and 5 days following axotomy or sham operation and perfused with 4% paraformaldehyde. Following fixation, the SCGs were removed, desheathed, cryoprotected in sucrose, embedded in OCT, and then sectioned on a cryostat at 10 μm. Sections were incubated for 1 h with rabbit anti-rat arg I (1:2000; Esch et al., 1998). A fluorescent donkey anti-rabbit secondary antibody (CY3, 1:250; Jackson ImmunoResearch Laboratories Inc., West Grove, PA) was used to detect the primary antibody. Both preabsorption of the rabbit anti-rat arg I antibody (1:2000) with 0.95 μg/μL recombinant arg I protein or omission of the primary antibody abolished all immunoreactivity. Monocytes and infiltrating macrophages were identified with the mouse monoclonal antibody ED-1 (1:100; Serotec, Oxford, UK; Dijkstra et al., 1985) and a biotinylated donkey anti-mouse secondary antiserum (1:200; Jackson ImmunoResearch Laboratories), which was visualized with Texas Red streptavidin (1:500; Jackson ImmunoResearch Laboratories). To double label ED-1 positive macrophages for arg I an Alexa Fluor 488 labeled goat anti-rabbit IgG (1:200; Molecular Probes) was used. Images were captured with a confocal scanning laser microscope LSM410 (Zeiss, Oberkochen, Germany). To confirm colocalization of ED-1 positive macrophages with arg I, the red and green images were superimposed in the RGB mode.

Polyamine Measurements

SCGs from intact, 5-day axotomized, or 5-day sham-operated adult male rats were harvested and immediately frozen on dry ice until use. Both SCGs from a single rat were pooled and homogenized in 50 μL of 1.5 *M* perchloric acid. After addition of 25 μL of 2 *M* potassium bicarbonate, samples were vortexed and centrifuged at 10,000 rpm for 1 min. Supernatant was sent on dry ice to Dr. G. Wu (Department of Animal Science, Texas A&M University) for measurement of polyamines by high-performance liquid chromatography (O'Quinn et al., 2002). Measurements were carried out on the SCGs from three animals per condition.

Statistics

Statistical measurements comparing two groups (e.g., axotomized vs. sham-operated SCGs) were done using a *t* test. Statistical measurements comparing three or more groups were done using one-way ANOVA and Bonferroni's post hoc *t* test. Differences in mean values were considered statistically significant if $p \leq 0.05$.

RESULTS

Changes in Gene Expression following Axotomy of the SCG

The Affymetrix RGU34A microarray contains 8799 probe sets specific for known rat genes and EST sequences. Certain genes and ESTs are represented by two or more different probe sets on the RGU34A array, allowing for validation of results for a particular gene or EST across multiple probe sets. Between 39 and 45% of all sequences spotted on the array were identified as present or marginally present in the sam-

ples from unoperated, sham-operated, or axotomized ganglia. A gene or EST was categorized as increased by axotomy (relative to sham) if it was called present or marginal in the axotomy sample, if the change call was increased or marginally increased, and if the calculated fold change was ≥2×. The change call (increased, marginally increased, no change, marginally decreased, or decreased) is a parameter determined by the MAS5.0 program based on statistical measurements of the signal log ratios for genes within a pairwise comparison. A gene can have a calculated fold change value of ≥2× with a change call of "no change," if statistical significance has not been reached for the comparative data. Similarly, a gene can be called "increased" even if the fold change is <2×. Therefore, we have required both statistical significance and a greater than 2× change to classify a gene as changed. For a decrease, the gene or EST had to be called present or marginal in the sham sample, the change call had to be decreased or marginally decreased, and the fold change had to be ≥2×. In addition, for both increases and decreases, changes ≥2× had to be observed for a given gene or EST in at least six out of the nine axotomy versus sham comparisons.

Using these criteria, the expression of 37 known genes (34 upregulated; 3 downregulated) and 23 ESTs (18 upregulated; 5 downregulated) was found to change at 6 h after axotomy (Appendices 1 and 2). Among the 37 known genes, 8 were shown to be regulated by multiple probe sets on the array (Appendix 1), whereas 12 were shown to be regulated by only one or two of the multiple probe sets representing that gene. At the 48-h postaxotomy time point, expression of 187 known genes (103 upregulated; 84 downregulated) and 131 ESTs (71 upregulated; 60 downregulated) was found to change (Appendices 1 and 2). Of the known genes, 34 were shown to be regulated by multiple probe sets (Appendix 1), whereas 26 were shown to be regulated by only one or two of the multiple probe sets. Lack of confirmation by multiple probe sets at both the 6- and 48-h postaxotomy time points may be due to low hybridization efficiency of some of those probe sets, resulting in the gene being called absent in samples applied to the chip. In fact, 24 of the 38 total unconfirmed changes were from probe sets that gave low hybridization signals, resulting in an absence call for that gene. Of the other 14 unconfirmed changes, the majority (12 out of 14) were for genes that exhibited fold changes close to the 2× cutoff criterion.

Figure 1 shows the correlation of average hybridization signal intensity for all 8799 sequences between two samples 6 h after a sham operation [Fig. 1(A)], between individual samples 6 h after axotomy and 6 h after a sham operation [Fig. 1(B)], between two samples 48 h after a sham operation [Fig. 1(C)], and between individual samples 48 h after axotomy and 48 h after a sham operation [Fig. 1(D)]. The increased degree of scatter in the graphs of axotomy versus sham SCGs [Fig. 1(B) and (D)] compared to the graphs of sham versus sham SCGs [Fig. 1(A) and (C)] is indicative of the observed axotomy-induced changes in gene expression. These changes comprised 0.68 and 3.6% of the total arrayed sequences at 6- and 48-h postaxotomy, respectively. The scatter seen in sham versus sham SCGs [Fig. 1(A) and (C)] does not represent significant differences in expression between sham SCGs, because the same differences are not reproducible across the other eight sham versus sham comparisons. Rather, this scatter represents a baseline degree of variability seen between any sham versus sham SCG pairing. No significant changes in gene expression were seen between sham-operated and intact control animals.

Known genes shown to change by microarray were categorized into the following functional groups: neuropeptides and cytokines, cell survival-related molecules, cell proliferation-related molecules, regulators of neurite outgrowth, neural transmission molecules, macrophage and inflammation molecules, transcription factors and chromosomal proteins, signal transduction molecules, extracellular matrix molecules, cytoskeletal elements, neurotrophin-related molecules, peptidases, metabolic molecules, and others. A complete list of genes and ESTs that changed ≥2× in ≥6 of 9 axotomy versus sham comparisons can be found in Appendices 1 and 2, respectively. A list of selected genes, their axotomy/sham fold change values at 6- and 48-h postaxotomy, and their functional categorization is shown in Table 1. Upregulated genes of particular interest fell predominantly into the categories of neuropeptides and cytokines, regulators of neurite outgrowth, cell survival-related molecules, cell proliferation-related molecules, macrophage and inflammation molecules, transcription factors and chromosomal proteins, and extracellular matrix molecules. Genes exhibiting the largest magnitude of increase coded for neuropeptides or cytokines, six of which were upregulated greater than 10×, and two of which were increased between 5 and 10×. Downregulated genes were predominantly neural transmission molecules or signal transduction molecules. Other categories were comprised more equally of both up- and downregulated genes.

Changes in Gene Expression following Decentralization of the SCG

Between 41 and 47% of all genes and ESTs spotted on the array were identified as present or marginally

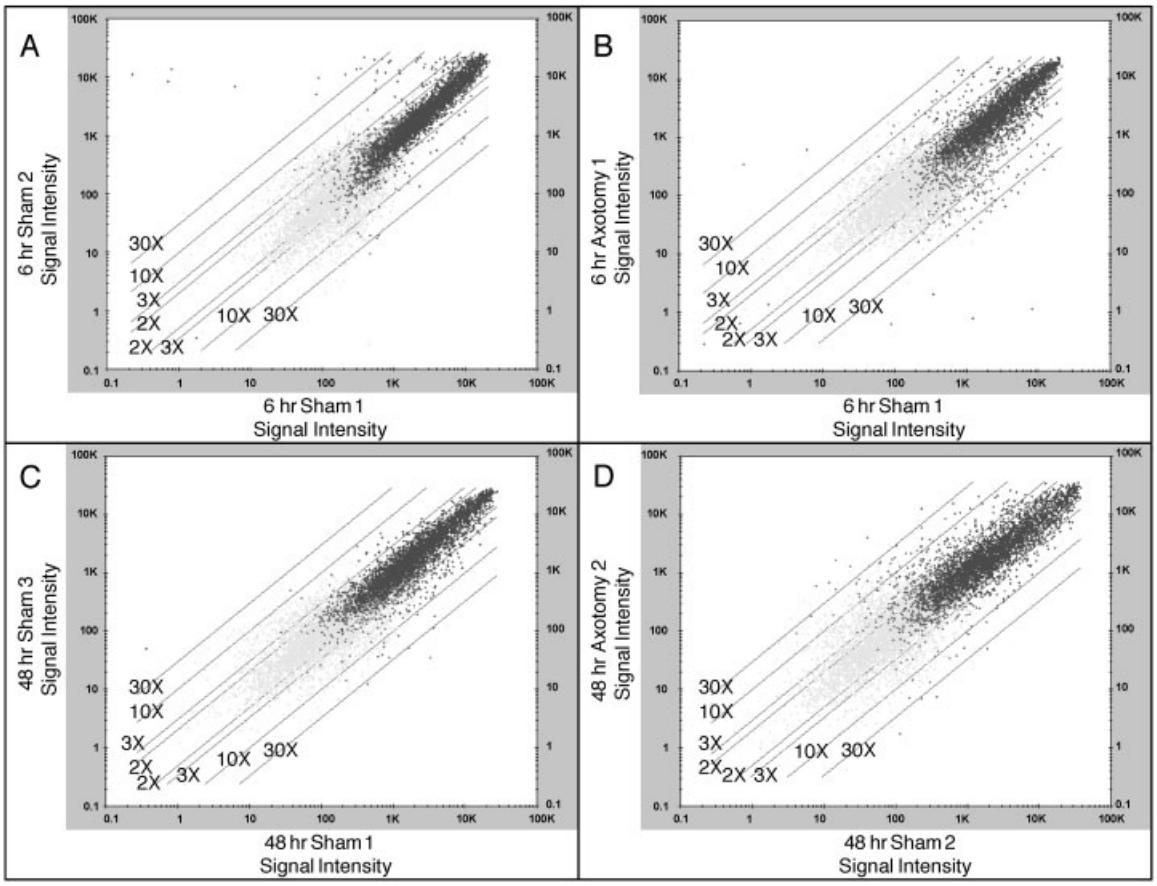

Figure 1 Correlation of hybridization signal intensity. The correlation of average hybridization signal intensities for all 8799 arrayed sequences between two samples 6 h after a sham operation (A), between individual samples 6 h after axotomy and 6 h after a sham operation (B), between two samples 48 h after a sham operation (C), and between individual samples 48 h after axotomy and 48 h after a sham operation (D) are shown. The dark gray points indicate those genes which were called present on at least one of the two microarray chips being compared. The lighter gray points indicate those genes that were called either marginal or absent on both of the chips being compared. The diagonal lines designate fold change boundaries as indicated. Spots appearing above the upper 2X change boundary line include genes or ESTs meeting criteria for axotomy-induced increases in expression, whereas spots appearing below the lower 2× boundary line include genes or ESTs meeting criteria for axotomy-induced decreases in expression.

present in the samples from decentralized ganglia. Six hours following decentralization, the expression of eight genes and five ESTs had increased ≥2× over the levels found 6 h after a sham operation (Table 2; ESTs not shown). Forty-eight hours postdecentralization, expression of two genes had increased ≥2× over 48-h postsham expression levels (Table 2). No genes were found to decrease at either 6- or 48-h postdecentralization, and no ESTs were found to either increase or decrease at 48 h postdecentralization. Interestingly, 9 of the 10 decentralization-regulated genes were also regulated by axotomy (Table 2). Calculation of axotomy/decentralization fold change values showed that, whereas five genes were upregulated similarly by axotomy and decentralization, four genes (MCP-1, osteopontin, RTI40, and galanin) were upregulated to a greater extent by axotomy than by decentralization (Table 2, column 3).

Time Course of Expression for Selected Genes following Axotomy

Because of material and cost limitations, not all postaxotomy time points of interest could be examined by microarray. Therefore, the expression of several genes of interest shown by microarray to increase following axotomy was further examined using real-time RT-PCR.

Table 1 Axotomy-Induced Changes in Gene Expression

Accession No.	Gene Name	6 h Ax/Sh	48 h Ax/Sh
	Peptides and Cytokines		
X01032	Cholecystokinin (CCK)	NC	31.9 (6)
M26745	Interleukin-6 (IL-6)	28.5 (9)	NC
M31603	Parathyroid hormone-related protein (PTHrP)$^{+P,+S}$	NC	19.6 (9)
J03624	Galanin	NC	19.3 (9)
X56306	Substance P (δ-Preprotachykinin)	NC	12.2 (6)
X02341	Vasoactive intestinal peptide (VIP)$^{+P,+S}$	NC	10.9 (9)
X80290	Pituitary adenylate cyclase activating polypeptide (PACAP)$^{+P,+S}$	NC	8 (9)
M15191	Substance P (β-Preprotachykinin)	NC	5.3 (8)
	Cell Survival-Related Molecules		
J02720	Arginase I^{+S}	NC	22.1 (9)
Y16188	Damage induced neuronal endopeptidase (DINE)$^{+S}$	NC	4.2 (7)
M11794	Metallothionein-1^{+S}	3.5 (8)	NC
M31837	Insulin-like growth factor binding protein 3^{+S}	NC	3.5 (8)
Z75029	Heat-shock protein 70 (HSP 70)$^{+S}$	3.4 (7)	NC
M91652	Glutamine synthetase^{+S}	NC	3.2 (7)
X75856	Bax inhibitor-1^{+S}	NC	2.6 (6)
Z24721	Superoxide dismutase^{+S}	NC	2.5 (6)
X63744	Glutamate/aspartate transporter^{+S}	NC	2.2 (8)
	Cell Proliferation-Related Molecules		
AA998164	Cyclin B1^{+P}	NC	18.1 (9)
M98049	Pancreatitis-associated protein (REG2)$^{+P,+S}$	NC	6.4 (6)
X60767	Cell division cycle control protein 2 (cdc2/p34)$^{+P}$	NC	4.7 (9)
X96437	P22/PACAP regulated gene (PRG1)/IEX-1^{+P}	3.2 (8)	3.2 (9)
	Regulators of Neurite Outgrowth		
J02720	Arginase I (stimulator)$^{+S}$	NC	22.1 (9)
M23566	Alpha 2-macroglobulin (stimulator)$^{+S}$	NC	8.3 (7)
Z54212	Epithelial membrane protein 1 (EMP1)/Progression associated protein (PAP) (stimulator)$^{+S}$	3.9 (6)	5.7 (7)
A03913	Protease nexin 1 (PN-1; stimulator)	NC	4.3 (7)
L46593	Small proline-rich protein (stimulator)	NC	4.3 (6)
M81642	Proteinase activated receptor 1/Thrombin receptor (inhibitor)	NC	−2.3 (9)
U49062	CD24/nectradin (inhibitor)	NC	−2.4 (7)
	Neural Transmission Molecules		
M27925	Synapsin 2	NC	−2.4 (8)
AF019974	Chromogranin B	NC	−2.5 (8)
AF033027	Prenylated SNARE protein	NC	−2.5 (8)
AF015304	Solute carrier family 29, member 1 (nucleoside transporter)	NC	−2.8 (9)
M93669	Secretogranin II	NC	−2.8 (9)
J05231	α5 Nicotinic acetylcholine receptor	NC	−2.9 (9)
AB003992	SNAP-25B	NC	−3 (9)
S45812	Monoamine oxidase A	NC	−3.1 (9)
M84648	Aromatic L-amino acid decarboxylase	NC	−3.2 (9)
L31621	α3 Nicotinic acetylcholine receptor	NC	−3.3 (9)
AB003991	SNAP-25A	NC	−3.3 (8)
X59132	Secretin receptor	NC	−4.5 (9)
U59672	Serotonin (5HT3) receptor	NC	−6.1 (9)
M22253	Sodium channel (Na 1.1)	NC	−35.3 (9)
	Macrophage and Inflammation Molecules		
M14656	Osteopontin$^{+P,+S}$	7.2 (9)	22.7 (9)
L18948	S100 calcium binding protein A9 (myeloid related protein 14)	12.8 (9)	NC
D11445	Gro	11.9 (9)	NC
X73371	Fc-gamma receptor II	3.4 (7)	11.5 (8)
X17053	MCP-1/JE	8.8 (9)	NC
J02722	Heme oxygenase-1	4.4 (9)	NC
D00913	Intercellular adhesion molecule 1 (ICAM-1)	3.4 (7)	NC
U90610	CXCR4 chemokine receptor	NC	−2.5 (9)
U16025	MHC class lb RT1	NC	−5.4 (9)

Table 1 (*Continued*)

Accession No.	Gene Name	6 h Ax/Sh	48 h Ax/Sh
	Transcription Factors and Chromosomal Proteins		
U50736	Cardiac adriamycin responsive protein (CARP)	NC	12.9 (9)
M18416	EGR1/Krox24/NGFI-A/ZIF268	12.1 (9)	NC
U78102	EGR2/Krox20	8.8 (9)	5 (8)
M63282	Activating transcription factor 3 (ATF-3)/Liver regeneration factor 1	5.1 (9)	7.9 (9)
AJ004858	Sox-11 (SYR-box containing gene 11)	NC	5.8 (9)
D84418	High mobility group box 2 (HMG2)	NC	5.7 (9)
M65149	C/EBP delta (CELF)	3.9 (9)	3.8 (7)
X06769	c-*fos*	3.4 (8)	NC
U04835	cAMP responsive element modulator (CREM)	NC	3 (9)
L26267	Nuclear factor kappa B p105 subunit	2.6 (6)	NC
	Signal Transduction Molecules		
M80367	Guanine nucleotide binding protein 2 (γ-interferon inducible)	7 (7)	6.1 (9)
M64092	cAMP-dependent protein kinase inhibitor, beta	NC	4.2 (9)
X58828	Protein tyrosine phosphatase, nonreceptor type 2	3.6 (6)	2.4 (9)
J05087	ATPase, Ca^{2+} transporting, plasma membrane 3	NC	−2.4 (9)
L14323	Phospholipase C-β1	NC	−3 (9)
L15556	Phospholipase C-β4	NC	−3.3 (9)
Z36276	cGMP-dependent protein kinase II	NC	−3.4 (9)
D45920	Inositol 1,4,5 triphosphate binding protein	NC	−3.5 (9)
J03754	ATPase, Ca^{2+} transporting, plasma membrane 2	NC	−4.2 (9)
D10666	Neural visinin-like Ca^{2+} binding protein	NC	−10 (9)
	Extracellular Matrix Molecules		
AI169327	Tissue inhibitor of metalloproteinase 1 (TIMP1)	6.3 (9)	7.1 (9)
L00191	Fibronectin	NC	4.5 (8)
AF072892	Versican V3	NC	3.5 (9)
S61865	Syndecan 1	NC	3.5 (9)
	Cytoskeletal Elements		
AF028784	Glial fibrillary acidic protein α and δ (GFAP)	5.5 (9)	5.5 (6)
AA892333	α tubulin	3.7 (6)	4.7 (9)
U30938	Microtubule-associated protein 2 (MAP-2)	NC	−2.3 (9)
Z12152	Neurofilament medium	NC	−3 (9)
AA818677	Neurofilament heavy	NC	−3.3 (9)
M25638	Neurofilament light	NC	−4.1 (9)
	Neurotrophin-Related Molecules		
X05137	p75, low-affinity neurotrophin receptor	NC	−2.6 (9)
M85214	TrkA	NC	−2.7 (9)
U88958	Neuritin	NC	−4.7 (9)
	Others		
AA892801	Eukaryotic translation elongation factor 2	NC	10.4 (6)
D38062	UDP-glucoronosyltransferase 1	NC	9.4 (9)

Axotomy/sham fold change values were calculated from microarray signal intensity data, as described in Materials and Methods. Shown here are the fold change values for a selected group of genes whose expression changed ≥2× following axotomy. Results are shown for both the 6-h and 48-h postaxotomy time points. Values represent the mean fold change for each gene across all of the nine axotomy/sham comparisons that exhibited a ≥2× change. The number in parentheses following each fold change value represents the number of axotomy/sham comparisons in which a ≥2× change in expression was seen. An entry of NC indicates that the expression of the gene did not meet the criteria for a change (see Results). Genes are categorized into functional groups. A number of genes could be listed under more than one functional category, and in fact, arg I is listed as both a cell-survival–related molecule and a regulator of neurite outgrowth. Genes with the designation of +S are positive stimulators of cell survival, whereas genes with the designation of +P stimulate cell cycle progression or are induced in proliferating cells.

These genes were ATF-3, arg I, cardiac ankyrin repeat protein (CARP), galanin, osteopontin, PACAP, parathyroid hormone-related peptide (PTHrP), and UDP-glucoronosyltransferase. Genes of interest were chosen based partly upon the magnitude of the increase and the consistency of the increase across all nine axotomy/sham comparisons. In addition, expression of several of these genes has been reported to be linked to regenerative processes and/or to increase after nerve injury in a different neural system. Such genes include arg I,

Table 2 Changes in Gene Expression Induced by Transection of the Cervical Sympathetic Trunks (CSTX)

Accession No.	Gene Name	6 h CSTX/Sh	6 h Ax/Sh	6 h Ax/CSTX
AF028784	Glial fibrillary acidic protein (GFAP) α and δ	5.4 ± 0.4 (9)	5.5 ± 0.5 (9)	NC
M80367	Guanine binding protein 2 (γ-interferon inducible)	4.4 ± 0.4 (6)	7 ± 1.8 (7)	NC
X17053	MCP-1/JE	3.5 ± 0.5 (6)	8.8 ± 1.5 (9)	3.8 ± 0.6 (8)
M11794	Metallothionein-1	3.1 ± 0.4 (7)	3.5 ± 0.3 (8)	NC
M14656	Osteopontin	3.1 ± 0.4 (7)	7.2 ± 1.2 (9)	3.7 ± 0.7 (6)
Z54212	Epithelial membrane protein 1 (EMP1)	2.8 ± 0.2 (9)	3.9 ± 0.3 (6)	NC
M65149	C/EBP delta (CELF)	2.8 ± 0.2 (9)	3.9 ± 0.2 (9)	NC
U92081	Epithelial cell transmembrane protein antigen/RT140	2.8 ± 0.2 (6)	5.7 ± 0.5 (8)	2.3 ± 0.1 (7)
		48 hr CSTX/Sh	48 hr Ax/Sh	48 hr Ax/CSTX
J03624	Galanin	3.6 ± 0.3 (6)	19.3 ± 3.7 (9)	7.3 ± 0.5 (9)
L11930	Cap1/Cyclase-associated protein homolog (MCH1)	2.4 ± 0.2 (6)	NC	NC

CSTX/sham values were calculated from microarray signal intensity data, as described in Materials and Methods. Shown here are the fold change values for all of the genes whose expression increased ≥2× at 6 h or 48 h following decentralization. For comparison, the axotomy/sham fold change values for each of these genes are shown as well. Values represent the mean fold change for each gene across all nine of the CSTX/sham or axotomy/sham comparisons that exhibited a ≥2× change. The number in parentheses following each fold change value represents the number of comparisons in which a ≥2× change in expression was seen. An entry of NC indicates that the expression of the gene did not meet the criteria for a change (see Results). No decreases in gene expression occurred following decentralization.

ATF-3, galanin, osteopontin, PACAP, and PTHrP (Holmes et al., 2000; Tsujino et al., 2000; Cai et al., 2002; Jander et al., 2002; Wang et al., 2002; Waschek, 2002). Importantly, real-time RT-PCR results validated the increases in expression seen by microarray for all genes examined.

Copy number of each gene of interest was calculated for unoperated, sham-operated, and axotomized conditions by comparison to standard curves generated from 10-fold serial dilutions of plasmid cDNAs. The time courses of changes in copy number are shown in Figures 2 and 3. Following axotomy, expression of four of the genes, arg I, ATF-3, galanin, and PTHrP, increased significantly above sham levels within 6–24 h after axotomy and remained high through 5 days postaxotomy (Fig. 2). Four additional genes, CARP, osteopontin, PACAP, and UDP-glucoronosyltransferase, were also significantly upregulated following axotomy. For these four genes, expression levels peaked at 24 h postaxotomy, followed by a decline in expression by 48 h (Fig. 3). Expression of PACAP and UDP-glucoronosyltransferase 48-h postaxotomy was not significantly increased relative to sham levels. In contrast, expression of CARP and osteopontin, though decreasing, was still significantly increased relative to sham at the 48 h and 5 days postaxotomy time points.

In addition to the calculation of absolute expression of genes of interest (in terms of copy number), relative expression of genes in axotomy and time-matched sham conditions was also calculated following normalization within each sample to expression of the ribosomal 18S gene, which was chosen as a housekeeping gene (Table 3). Expression of ribosomal 18S did not differ significantly at any time point following axotomy or sham surgery from the levels seen in unoperated animals (data not shown). Axotomy/sham fold change values obtained by RT-PCR closely paralleled axotomy-induced changes in copy number, as expected. In addition, axotomy/sham fold change values obtained by RT-PCR showed the same trends in gene expression as did the microarray (Table 3). For five of the genes (i.e., arg I, CARP, galanin, LIF, and UDP-glucoronosyltransferase), RT-PCR indicated a change in gene expression ≥2× at the 6 h postaxotomy time point, whereas microarray indicated no change. This may reflect a greater sensitivity of the amplification-based PCR method over the hybridization-based technique of the microarray. In keeping with this idea, all five of these genes had been called absent in all samples at the 6 h time point by microarray analysis due to low hybridization signal intensity levels. This suggests that in instances when copy number of a given gene is extremely low, the microarray technique is not sensitive enough to detect transcripts, despite a significant upregulation upon experimental treatment.

As noted by microarray analysis, no genes or ESTs had been shown to change following sham surgery (sham vs. unoperated comparisons). In addition, expression of the majority of genes examined by real-time RT-PCR was also found not to be affected by sham surgery. However, three genes, arg I, osteopontin, and

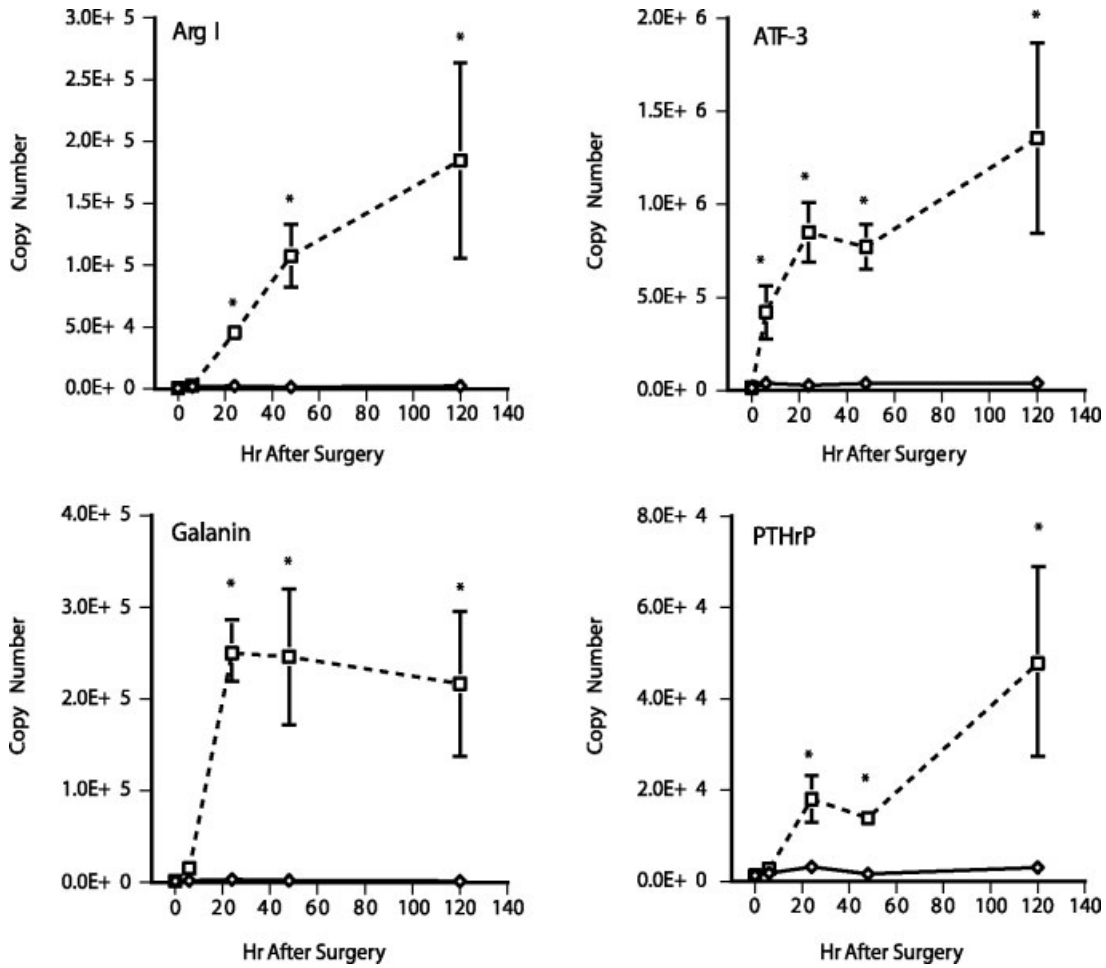

Figure 2 Time course of expression for genes that remain highly elevated at 5 days after axotomy. Real-time RT-PCR was used to measure levels of expression for selected genes of interest in axotomized, time-matched sham control, and unoperated SCGs. Whereas ATF-3 expression increased significantly within 6 h following axotomy, expression of arg I, galanin, and PTHrP did not increase significantly relative to sham until 24 h after axotomy. Expression of all four genes remained high through 5 days postaxotomy. Copy number was calculated as described in Materials and Methods and is shown here as a function of time (hours) following axotomy (squares) or sham surgery (diamonds). The values for intact animals are shown at time = 0. Each point represents the mean copy number ± SEM from four animals. Where error bars are not depicted, the error was too small to be shown graphically. Asterisks indicate significant differences in copy number between axotomy and time-matched sham SCGs ($p \leq 0.05$). Copy number values for all conditions were greater than 0, although copy number for all four genes was low in sham-operated and unoperated SCGs.

PACAP, were found by real-time RT-PCR to increase following sham surgery, although due to the scale of the graphs in Figures 2 and 3, these increases are not evident. Arg I and PACAP increased about 5× within 6 h following sham surgery, and remained higher than unoperated levels through 5 days. Osteopontin initially increased 4.7× over unoperated levels within 6 h postsham surgery but returned to unoperated levels by 24 h. Despite sham-induced increases for these three genes, axotomy induced dramatic increases in expression above sham levels (Figs. 2 and 3, Table 3).

Time Course of Expression of LIF following Axotomy

Microarray analysis did not reveal an axotomy-induced increase in leukemia inhibitory factor (LIF; see Table 3), although our previous research had indicated that this cytokine is upregulated within the SCG by 6 h after axotomy (Sun et al., 1994; Sun and Zigmond, 1996a). In fact, LIF was called absent in all samples by microarray analysis. Therefore, we decided to reexamine the regulation of LIF using real-time RT-PCR. Low but detect-

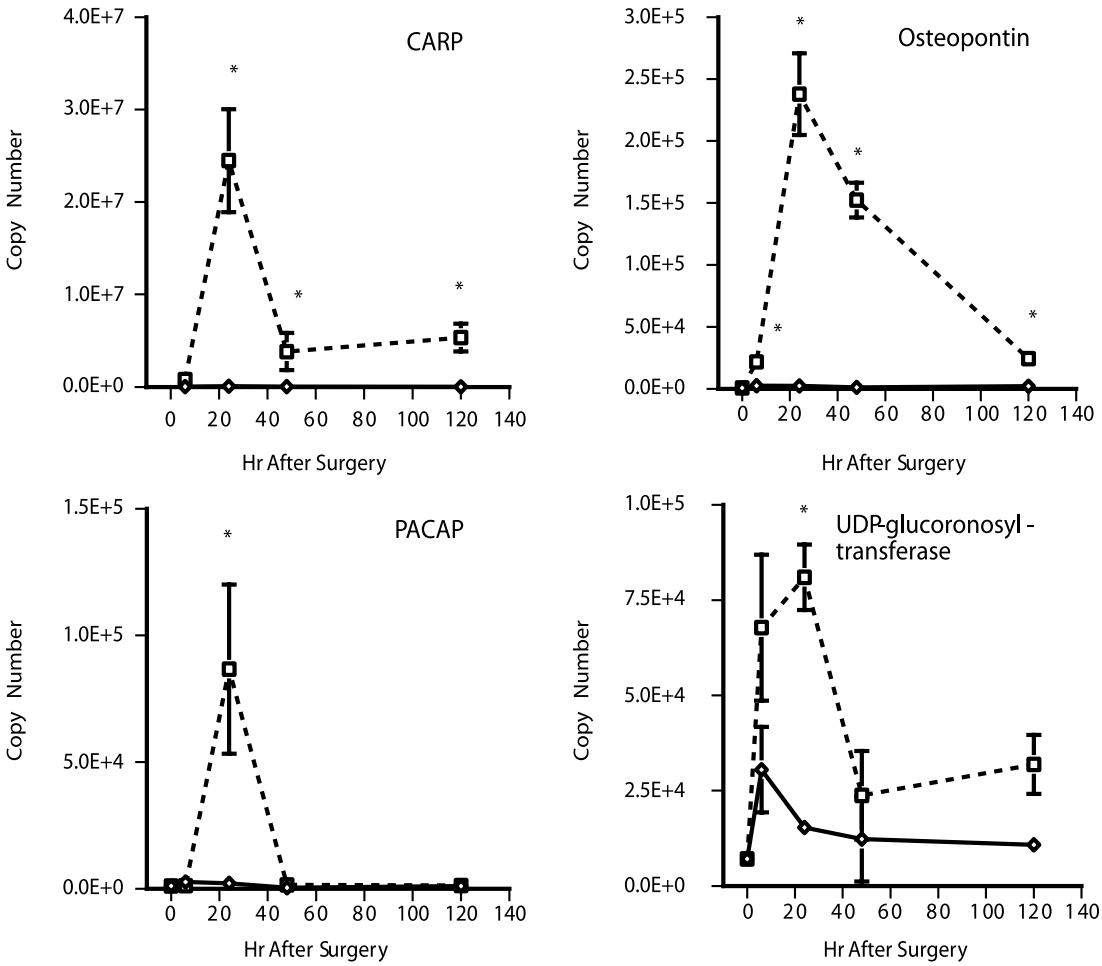

Figure 3 Time course of expression for genes whose expression peaks early after axotomy. Real-time RT-PCR was used to measure levels of expression for selected genes of interest in axotomized, time-matched sham control, and unoperated SCGs. Expression of four genes, CARP, osteopontin, PACAP, and UDP-glucoronosyltransferase, was shown to increase rapidly and significantly following axotomy, peaking at 24 h. Subsequently, expression levels rapidly decreased, although expression of CARP and osteopontin was still significantly increased relative to sham at the 5-day time point. Copy number was calculated as described in Materials and Methods, and is shown here as a function of time (hours) following axotomy (squares) or sham surgery (diamonds). The values for intact animals are shown at time = 0. Each point represents the mean copy number ± SEM from four animals. Where error bars are not depicted, the error was too small to be shown graphically. Asterisks indicate significant differences in copy number between axotomy and time-matched sham SCGs ($p \leq 0.05$). Copy number values under all conditions were greater than 0. CARP copy number was not measured in intact control animals.

able levels of LIF were found in unoperated and sham-operated ganglia by this technique (35–115 copies/animal). Axotomy increased LIF expression >750-fold within 6 h (Fig. 4). Expression was still dramatically increased (>160-fold) relative to that in sham-operated ganglia at 24 h postaxotomy, but by 48 h there was no significant difference between the two groups (Fig. 4). These data are in agreement with our previous results obtained by Northern blot analysis (Sun and Zigmond, 1996a).

Arg I mRNA Is Upregulated following Axotomy in Neurons

Due to its neurite outgrowth promoting and anti-apoptotic actions (Dawson et al., 1991; Esch et al., 1998; Cai et al., 2002), we examined further the expression of arg I mRNA after axotomy using *in situ* hybridization. Forty-eight hours following axotomy, many neurons in the SCG were labeled (Fig. 5C); in contrast, labeled neurons were not found 6

Table 3 Comparison of RT-PCR and Microarray Fold Change Data

	Fold Change (Axotomy/Sham)					
	Real-Time RT-PCR				Microarray	
Gene	6 h	24 h	48 h	5 Day	6 h	48 h
Arg I	2.9 ± 0.8	17.8 ± 3.9	37.7 ± 8	30 ± 8.8	NC	22.1 ± 6.3
ATF-3	21.8 ± 12.6	29.4 ± 3.2	22.7 ± 5.5	31.3 ± 12.2	5.1 ± 0.3	7.9 ± 1.5
CARP	10.7 ± 4.6	636.7 ± 94.6	156.1 ± 31.7	195.5 ± 42.4	NC	12.9 ± 2
Galanin	4.8 ± 3	46.5 ± 6.7	60.9 ± 15.5	38.8 ± 1	NC	19.3 ± 3.7
LIF	773.5 ± 510.8	166.1 ± 88.2	NC	NC	NC	NC
Osteopontin	18.5 ± 2.4	143.9 ± 19.9	78 ± 2.9	7 ± 1.6	7.1 ± 1.2	22.7 ± 5.9
PACAP	NC	33.9 ± 12.7	2.1 ± 0.7	NC	NC	8 ± 1
PTHrP	NC	8.6 ± 1.5	5.1 ± 0.5	8.1 ± 3.3	NC	19.6 ± 7.6
UDP-Glucoronosyltransferase	3.8 ± 1	11.3 ± 3.9	4.3 ± 1.4	7.6 ± 5.3	NC	9.4 ± 2.9

Real time RT-PCR was used to measure levels of expression for selected genes in axotomized and time-matched sham-operated SCGs. Axotomy/sham fold change values were calculated following normalization to the level of expression of a housekeeping gene, ribosomal 18S, as described in Materials and Methods. Fold change values ± SEM are shown for 6-, 24-, 48-h, and 5-day postaxotomy time points. Four animals were examined for each condition. For comparison, the axotomy/sham fold change values calculated from the 6- and 48-h microarray data are also shown. An entry of NC indicates that the expression of the gene did not meet the criteria for a change (see Results).

or 48 h after a sham operation [Fig. 5(B) and (D)], 6 h following axotomy [Fig. 5(A)], or in unoperated animals (data not shown). The labeled neurons were somewhat more concentrated in the caudal and middle thirds of the ganglion near the CST and ECN, respectively, with a diminished labeling in the rostal third near the ICN. Labeled cells were not seen in any conditions when sections were exposed to a sense probe or to hybridization buffer without any probe (data not shown).

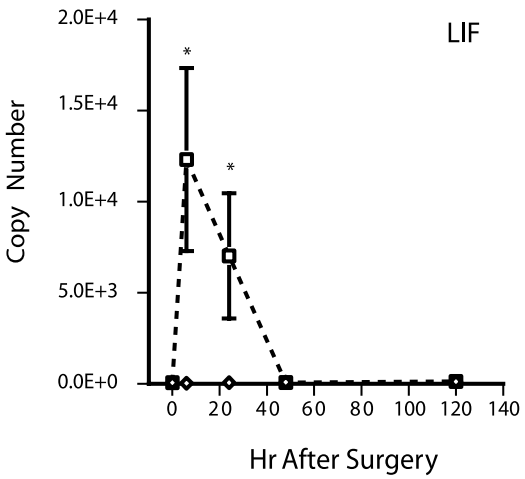

Figure 4 Time course of expression of LIF after axotomy. LIF expression after axotomy was measured by real-time RT-PCR. LIF increased rapidly and significantly within 6 h following axotomy. Expression remained significantly increased at 24 h postaxotomy, but returned to sham levels by 48 h. Copy number was calculated as described in Materials and Methods, and is shown here as a function of time (hours) following axotomy (squares) or sham surgery (diamonds). The values for intact animals are shown at time = 0. Each point represents the mean copy number ± SEM from four animals. Where error bars are not depicted, the error was too small to be shown graphically. Asterisks indicate significant differences in copy number between axotomy and time-matched sham SCGs ($p \leq 0.05$). Copy number values under all conditions were greater than 0, although copy number was low in sham-operated and unoperated SCGs.

Arg I Protein Is Upregulated following Axotomy and Is Localized to Neurons and Macrophages

To determine whether axotomy caused an increase in the level of arg I protein, Western blot analysis was performed on extracts from SCGs 48 h after axotomy or a sham operation. A band corresponding to the predicted molecular weight of arg I (i.e., 43 kDa) was present in the axotomized but not in the sham-operated control samples (Fig. 6). Next, immunohistochemistry was used to localize the arginase-expressing cells within the SCG. No immunopositive cells were detected in sections taken from sham-operated ganglia [Fig. 7(C)]; however, a large number of highly immunoreactive cells were seen in sections taken from ganglia 2 days [Fig. 7(A)] and 5 days (data not shown) after axotomy. The majority of these labeled cells were neurons, and they were widely distributed within the SCG but were less plentiful in the region near the ICN [Fig. 7(A) and (B)]. In addition, a second population of smaller immunopositive cells was located at the exit points of the two major postganglionic trunks, the ICN and ECN [Fig. 7(A) and (E)]. These smaller cells in the nerve roots were also labeled by the macrophage-recognizing antibody, ED-1 [Fig. 7(E)]. Interestingly, ED-1 labeled macrophages within the body of the SCG were not arg I positive [Fig. 7(D)].

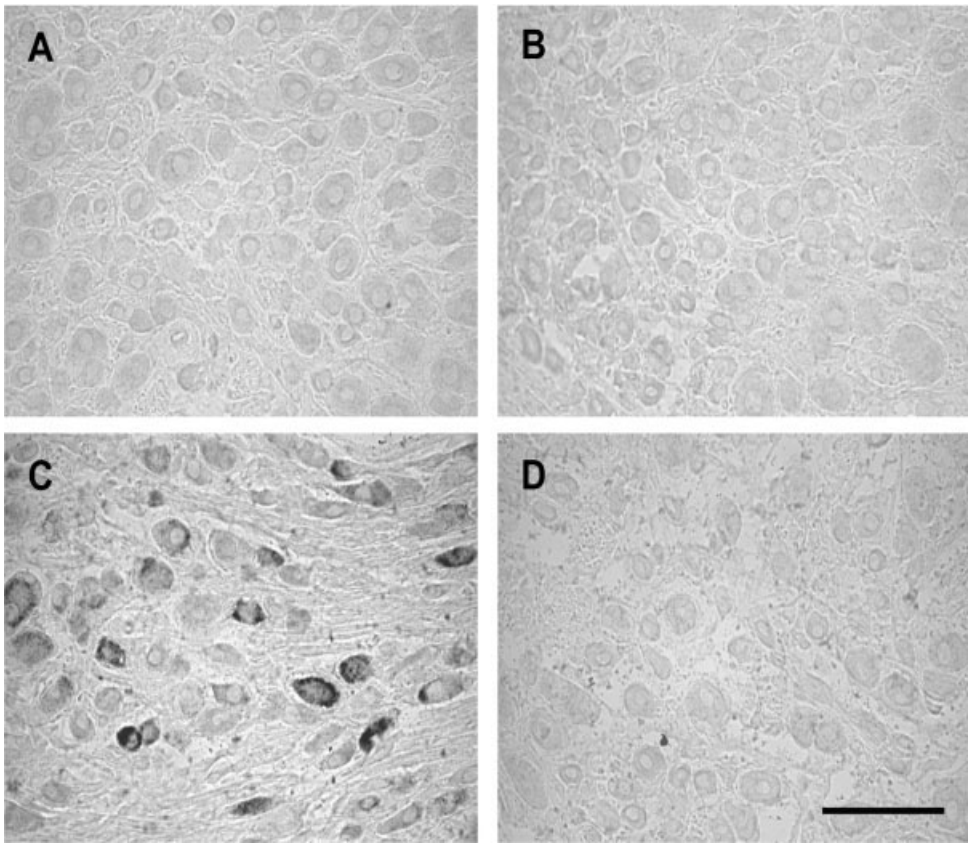

Figure 5 *In situ* hybridization for arg I in the rat SCG after axotomy. Sections were hybridized to a digoxigenin-labeled antisense probe to arg I 6 h (A) or 2 days (C) after axotomy or 6 h (B) or 2 days (D) after a sham operation. No labeled neurons were found under any condition when sections were hybridized to sense probes (data not shown). The scale bar equals 50 μm.

Upregulation of Polyamines following Axotomy

The diamine putrescine and the polyamines spermidine and spermine are produced downstream of the actions of the enzymes arg I and ornithine decarboxylase, and have been postulated to promote neurite outgrowth (Dornay et al., 1986; Gilad et al., 1996; Cai et al., 2002). Therefore, the levels of putrescine, spermidine, and spermine in the SCGs of intact, axotomized, and sham-operated rats were measured by high-performance liquid chromatography. Five days after surgery, putrescine had increased 3.6-fold [Fig. 8(A)] and spermidine, 3.1-fold [Fig. 8(B)] in axotomized ganglia compared to sham-operated control ganglia. In contrast, there was no significant change in the levels of spermine following axotomy [Fig. 8(C)] and no differences in the levels of any of the compounds between unoperated and sham-operated ganglia [Fig. 8(A)–(C)].

DISCUSSION

Although the importance of changes in mRNA and protein synthesis for regeneration has long been recognized (e.g., Watson, 1974; Smith and Skene, 1997), knowledge of the identities of the affected genes has been rudimentary. Using a gene microarray approach, we determined the changes in gene expression that occur in the SCG following transection of its postganglionic nerve trunks. We observed both increases and decreases in gene expression**.** A large number of downregulated genes were categorized as molecules involved in neural transmission, which is of interest, given that this is a cell population in which transmission has been halted. These included transmitter receptors, enzymes involved in transmitter synthesis and degradation, synaptic vesicle proteins, and a sodium channel. Many decreases were also seen in signal transduction molecules. The list of genes whose expression increased after axotomy provides candidates for proteins promoting sympathetic nerve

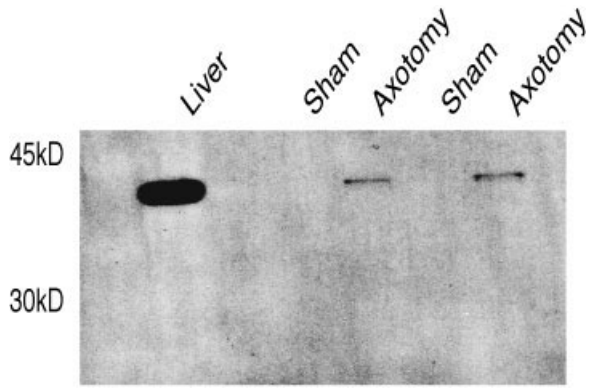

Figure 6 Western blot analysis of arg I in the rat SCG two days after axotomy. A strong signal is detected in the rat liver extract at 43 kDa, which comigrates with recombinant arginase (data not shown). Each SCG extract was made from the two ganglia from a different rat. No detectable arg I was found in extracts from ganglia 48 h after a sham operation. Arg I was detected in extracts from ganglia 48 h following axotomy.

regeneration. The largest and most consistent increases in expression were for genes coding for neuropeptides and cytokines.

The upregulation of certain neuropeptides [i.e., galanin, vasoactive intestinal polypeptide (VIP), PACAP, and substance P] following nerve injury has been reported previously in sensory and sympathetic systems (Hyatt-Sachs et al., 1993; Rao et al., 1993b; Mohney et al., 1994; Schreiber et al., 1994; Zhang et al., 1994; Moller et al., 1997). Microarray analysis of gene expression in the axotomized SCG not only verified the already documented upregulation of these neuropeptides (thus providing validation for the microarray approach), but also identified two additional upregulated neuropeptides, cholecystokinin (CCK) and PTHrP. In addition, microarray analysis revealed that the increases in neuropeptide expression are among the most dramatic noted in the axotomized ganglion, suggesting that these molecules play a major role in peripheral nerve regeneration. At present, direct evidence for a function in regeneration exists only for galanin. Using a functional assay for recovery after sciatic nerve injury, a substantial delay of several weeks in nerve regeneration was found in galanin knockout mice (Holmes et al., 2000). Furthermore, reduced neurite outgrowth was found in sensory neurons cultured from these animals (Holmes et al., 2000), and this phenotype was rescued by addition of galanin (Mahoney et al., 2003). Experiments to determine whether galanin is also important for sympathetic nerve regeneration are in progress. Although there is currently no comparable evidence that VIP and/or PACAP affect peripheral nerve regeneration, the results of several developmental studies make such hypotheses attractive. For example, PACAP and VIP increase survival and neurite extension of sympathetic neuroblasts (DiCicco-Bloom et al., 2000), and VIP increases survival of cultured sympathetic neurons deprived of NGF (Tanaka and Koike, 1994), a condition similar to that faced by neurons *in vivo* after axotomy. In addition to affecting neurons, VIP can also act on Schwann cells to increase the secretion of laminin (Q.L. Zhang et al., 1996), and on "resting" macrophages to stimulate the expression of IL-6 (Martinez et al., 1998).

Our microarray data revealed increases in expression of two additional neuropeptides, cholecystokinin (CCK) and PTHrP, which had not previously been reported to be present in sympathetic neurons. It is of interest, therefore, that systemic administration of CCK increases sympathetic nerve regeneration after treatment with the neurotoxin 6-hydroxydopamine (Manni et al., 2001). Although nothing is known about the effects of PTHrP in the injured peripheral nervous system, this neuropeptide is induced by reactive astrocytes after brain injury produced by a stab wound, and has been proposed as a mediator of inflammation (Funk et al., 2001). Knowledge of the dramatic upregulation of numerous neuropeptides following nerve injury underscores the need to examine specific actions of the neuropeptides during regeneration.

Because axonal regrowth is essential for functional recovery following axotomy, it is noteworthy that several of the axotomy-regulated genes identified in the microarray screen have previously been shown to affect neurite outgrowth. The expression of four genes that promote neurite outgrowth (arg I, protease nexin-1, small proline-rich repeat peptide, and alpha 2-macroglobulin) increased, while that of two genes that inhibit neurite outgrowth (CD24/nectradin and the thrombin receptor) decreased (Zurn et al., 1988; Mori et al., 1990; Monard, 1993; Shewan et al., 1996; Bonilla et al., 2002; Cai et al., 2002). Interestingly, protease nexin-1 (PN-1) acts to inhibit thrombin (Monard, 1993; Festoff et al., 1996). Therefore, the inhibitory effects of thrombin on neurite outgrowth might be overcome by both upregulation of its inhibitor and downregulation of its receptor. These changes in expression of neurite outgrowth-related molecules support the idea of a switch in gene expression after axotomy to favor axonal outgrowth.

Of particular interest among the upregulated neurite outgrowth-promoting genes is arg I, an enzyme that catalyzes the hydrolysis of arginine to ornithine and urea. Ornithine can be converted to the diamine putrescine, and then to the polyamines spermidine and spermine through the sequential actions of ornithine

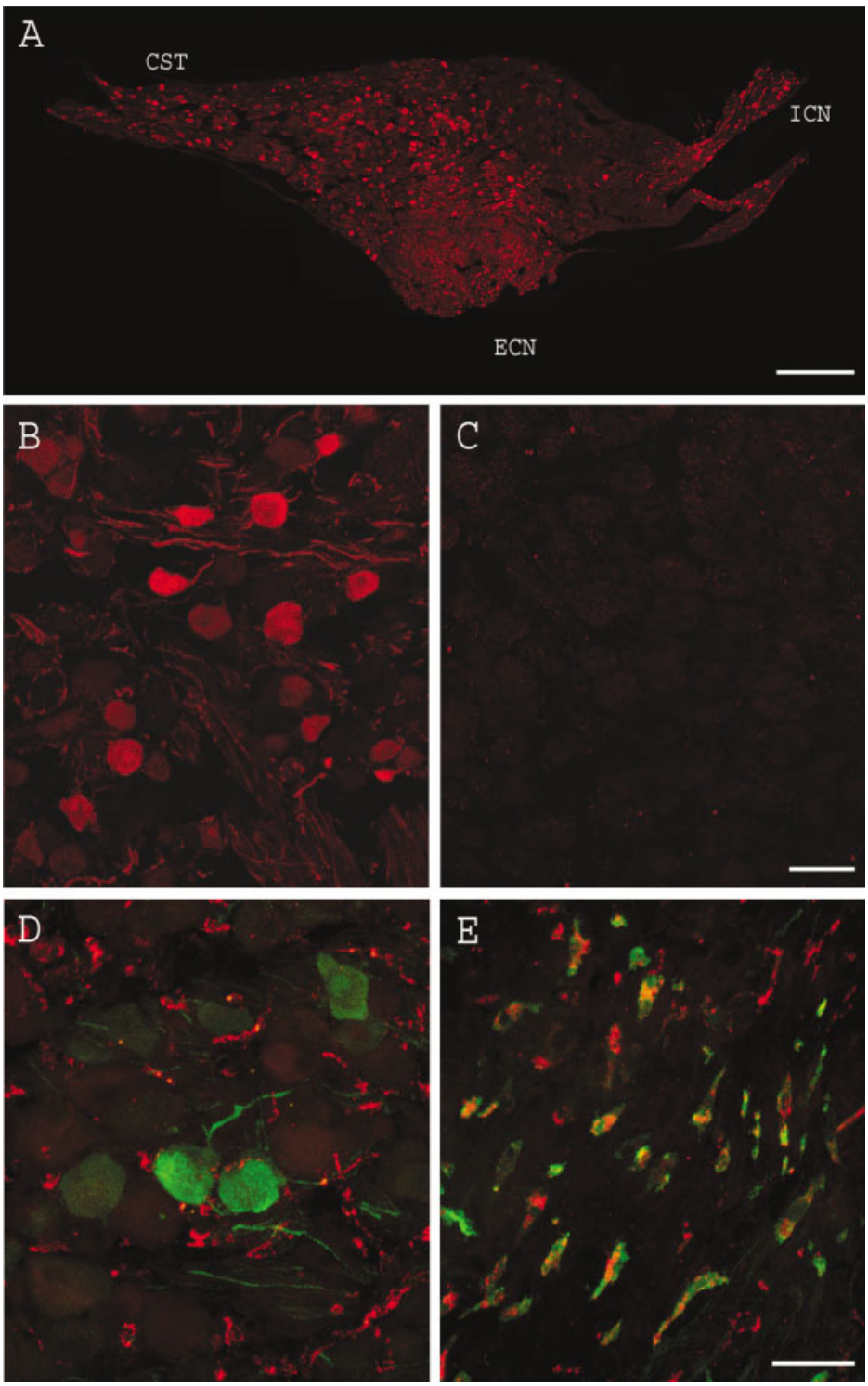

Figure 7 Immunohistochemistry for arg I in the rat SCG 2 days after axotomy. Low magnification montage shows the distribution of arg I staining (A). Arg I is localized to neurons and their processes within the ganglion (A,B) and to a small cell population within the postganglionic nerve trunks of the internal and external carotid nerves (ECN and ICN, A). No immunopositive labeling was seen in sections from sham-operated (C) or intact animals (data not shown). Immunohistochemical experiments identified the small arg I-positive cells within the postganglionic nerve trunks to be ED-1 positive macrophages (E). ED-1 positive macrophages within the ganglion were not arg I-positive (D). Arg I = red (A,B,C). Arg I = green (D,E). ED-1 = red (D,E). CST, cervical sympathetic trunk. Scale bars equal 500 μm (A), 50 μm (B,C), and 50 μm (D,E).

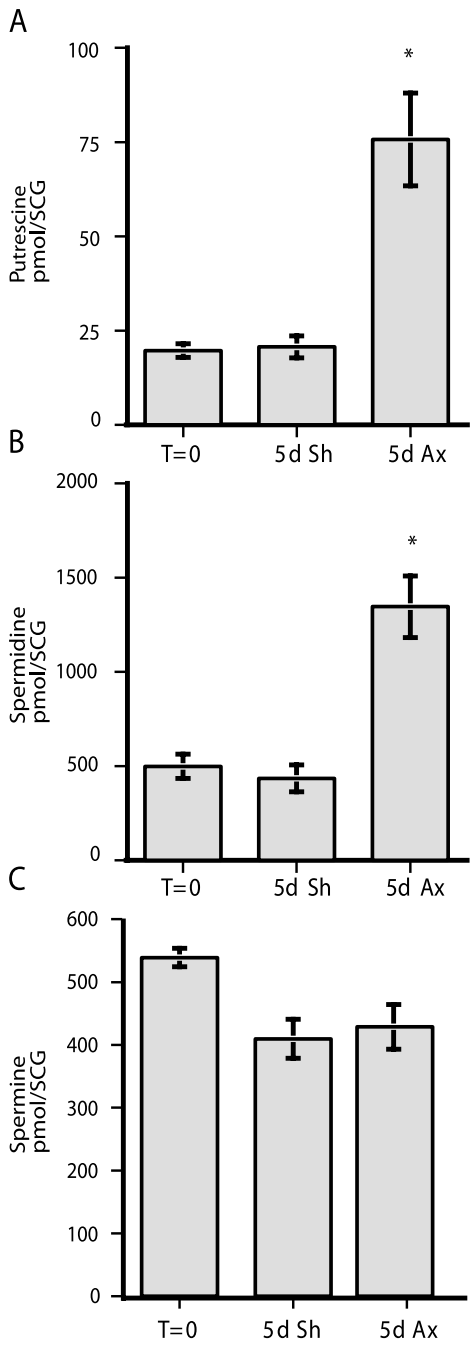

Figure 8 Axotomy-induced increases in putrescine and spermidine. The diamine putrescine and the polyamines spermidine and spermine were measured by HPLC in 5-day axotomized SCGs (5d Ax), 5-day sham-operated control SCGs (5d Sh), and unoperated SCGs (T =0). Levels of putrescine and spermidine increased 3.6× (A) and 3.1× (B), respectively, after axotomy compared to after sham surgery (n = 3 animals/condition). Asterisks indicate statistically significant changes (p = 0.05). No axotomy-induced change was seen in spermine levels. In addition, no significant difference was seen between sham and unoperated control SCGs for putrescine, spermidine, or spermine levels.

decarboxylase (ODC), spermidine synthase, and spermine synthase (Seiler, 2000). Although expression of ODC, a rate-limiting enzyme in polyamine biosynthesis, remains unchanged following SCG axotomy (as determined by our microarray analysis), its activity increases (Gilad and Gilad, 1983). In addition, increases in arginase expression have been associated with increased polyamine synthesis (Kepka-Lenhart et al, 2000; Li et al, 2002). Treatment with exogenous polyamines accelerates neurite outgrowth and functional recovery following *in vivo* axotomy of adult rat SCG neurons and facial motoneurons (Dornay et al., 1986; Gilad et al., 1996). Recent work by Cai et al. (2002) has shown that upregulation of arg I and the subsequent increase in polyamines are sufficient to promote axonal outgrowth from cultured postnatal CNS neurons grown on the normally inhibitory substrates of myelin-associated glycoprotein or myelin. We have now reported an upregulation of arg I, putrescine, and spermidine in the injured PNS. The axotomy-induced increases in arg I mRNA and protein and in putrescine and spermidine indicate a potential role for arg I and the polyamines in sympathetic nerve regeneration, presumably by promoting axonal outgrowth.

In addition to a putative neurite outgrowth-promoting role, arg I has an antiapoptotic effect on cortical neurons in culture (Esch et al., 1998). Although rapid cell death is widespread in neonatal peripheral neurons after axotomy, it is rarer in adult peripheral neurons. For example, there was no neuronal loss in the adult guinea pig SCG during the first week after postganglionic nerve crush, although a decrease occurred by 1 month (Purves, 1975). It is noteworthy, therefore, that arg I and a number of other genes encoding antiapoptotic proteins were upregulated in the axotomized SCG. These include Bax inhibitor-1, superoxide dismutase, damage-induced neuronal endopeptidase (DINE), and metallothionein-1 (Gorman et al., 1996; Jean et al., 1999; Kiryu-Seo et al., 2000; Giralt et al., 2002). Whether these gene products contribute to the survival of axotomized SCG neurons remains to be elucidated.

Given the cellular heterogeneity of the SCG, it is reasonable to expect that axotomy has an effect not only on the SCG neurons, but also on their associated nonneuronal cells. An example of this influence is the induced proliferation of glial cells (satellite cells and Schwann cells) and resident macrophages by 2 days postaxotomy (Schreiber et al., 2002; M. Bachoo, A.K. Hall., U. Vaidyanathan, and R.E. Zigmond, unpublished observations). This proliferative effect may be driven by changes in gene expression within nonneuronal cells. Microarray analysis has revealed an axotomy-induced increase in several cell cycle-associated

molecules, including cdc2, cyclin B, and the Schwann cell mitogen Reg-2 (Livesey et al., 1997). Therefore, it will be of interest to determine the cellular localization of these upregulated genes. Previous work has shown altered expression of other genes within nonneuronal cells of the SCG. For example, LIF is upregulated in nonneuronal cells of the rat SCG within 6 h postaxotomy (Sun et al., 1994), and heme oxygenase-1 increases in glial cells and macrophages (Magnusson and Kanje, 1998; Magnusson et al., 2000). In addition, glial fibrillary acidic protein (GFAP) is upregulated in satellite/Schwann cells of the axotomized SCG in guinea pigs (Elfvin et al., 1987). For many of the upregulated genes identified by microarray, the cell type in which the upregulation occurs remains to be determined. Such information will aid in formulating hypotheses concerning the function of upregulated molecules during regeneration.

The more global approach afforded by microarray technology allows for identification of molecules comprising potential pathways activated upon nerve injury. In fact, some of the changes in gene expression revealed in the microarray screen may represent cascades of biochemical events, as previous studies have reported links between many of the upregulated genes. For example, evidence supports the idea that LIF, a cytokine that is rapidly upregulated after axotomy (Fig. 4; Banner and Patterson, 1994; Sun et al., 1994), is required for the axotomy-induced upregulation of later appearing genes, including galanin, VIP, substance P (Rao et al., 1993a; Corness et al., 1996; Sun and Zigmond, 1996a, 1996b), Reg-2, and DINE (Livesey et al., 1997; Kato et al., 2002). DINE, in turn, leads to increased expression of superoxide dismutase (Kato et al., 2002). A second axotomy-induced cytokine, IL-6, has been implicated in the axotomy-induced expression of galanin in sensory neurons and of TIMP1 (tissue inhibitor of metalloproteinases-1) in fibroblasts (Sato et al., 1990; Thompson et al., 1998). Cascades may also result from PACAP's ability to induce expression of the glutamate/aspartate transporter, glutamine synthetase, and the PACAP-regulated gene (PRG1; Schafer et al., 1996; Figiel and Engele, 2000), and from VIP's ability to induce PN-1 expression (Bleuel et al., 1995) and to stimulate its secretion (Festoff et al., 1996). Identification of the molecular players of such pathways by microarray now allows for the further characterization of those pathways in the context of regeneration.

Recently, two studies using Affymetrix microarrays have been published on changes in gene expression in dorsal root ganglia after sciatic nerve transection or spinal nerve ligation (Costigan et al., 2002; Wang et al., 2002). Over 40 of the changes in gene expression reported in each of these studies mirrored the changes seen in the axotomized SCG. Among the changes seen in all three studies were increases in expression of a number of genes associated with inflammation, namely allograft inflammatory factor-1, alpha 2-macroglobulin, complement protein C1q beta chain, and Fc-gamma receptor.

In contrast to the effects of axotomy, no changes in gene expression were seen by microarray as a result of sham surgery. In addition, the expression of only 10 genes changed when the predominantly preganglionic cervical sympathetic trunk (CST) was transected (decentralization). With the exception of Cap1, a molecule involved in actin polymerization, these genes were also upregulated to a similar or greater extent by axotomy (Table 2). Because the CST contains axons of a small number of neurons located in the caudal part of the SCG (Bowers and Zigmond, 1979), some of the changes that result from this lesion could actually be the consequences of axotomizing those neurons rather than decentralization. Such an explanation has been previously proposed for the increase in galanin mRNA after CST transection (Mohney et al., 1994). The striking difference in the response of cells in the ganglion to decentralization and to axotomy highlights the latter as an attractive system for future studies on the mechanisms underlying plasticity in gene expression in the nervous system. The ultimate goal of such studies would be to elucidate the cascade of biochemical events that lead from peripheral nerve injury to regeneration.

We thank Maryanne Pendergast for her assistance with the confocal microscopy.

REFERENCES

Banner LR, Patterson PH. 1994. Major changes in the expression of the mRNAs for cholinergic differentiation factor/leukemia inhibitory factor and its receptor after injury to adult peripheral nerves and ganglia. Proc Natl Acad Sci USA 19:7109–7113.

Bleuel A, de Gasparo M, Whitebread S, Puttner I, Monard D. 1995. Regulation of protease nexin-I expression in cultured Schwann cells is mediated by angiotensin II receptors. J Neurosci 15:750–761.

Bonilla IE, Tanabe K, Strittmatter SM. 2002. Small proline-rich repeat protein 1A is expressed by axotomized neurons and promotes axonal outgrowth. J Neurosci 22: 1303–1315.

Bowers CW, Zigmond RE. 1979. Localization of neurons in the rat superior cervical ganglion that project into different postganglionic trunks. J Comp Neurol 185:381–391.

Cai D, Deng K, Mellado W, Lee J, Ratan RR, Filbin MT. 2002. Arginase I and polyamines act downstream from

cyclic AMP in overcoming inhibition of axonal growth by MAG and myelin in vitro. Neuron 15:711–719.

Cheah TB, Geffen LB. 1973. Effects of axonal injury on norepinephrine, tyrosine hydroxylase and monoamine oxidase levels in sympathetic ganglia. J Neurobiol 4:443–452.

Corness J, Shi TJ, Xu ZQ, Brulet P, Hokfelt T. 1996. Influence of leukemia inhibitory factor on galanin/GMAP and neuropeptide Y expression in mouse primary sensory neurons after axotomy. Exp Brain Res 112:79–88.

Costigan M, Befort K, Karchewski L, Griffin RS, D'Urso D, Allchorne A, Sitarski J, Mannion JW, Pratt RE, Woolf CJ. 2002. Replicate high-density rat genome oligonucleotide microarrays reveal hundreds of regulated genes in the dorsal root ganglion after peripheral nerve injury. BMC Neurosci 3:16.

Dawson VL, Dawson TM, London ED, Bredt DS, Snyder SH. 1991. Nitric oxide mediates glutamate neurotoxicity in primary cortical cultures. Proc Natl Acad Sci USA 88:6368–6371.

De Leon M, Welcher AA, Suter U, Shooter EM. 1991. Identification of transcriptionally regulated genes after sciatic nerve injury. J Neurosci Res 29:437–448.

DiCicco-Bloom E, Deutsch PJ, Maltzman J, Zhang J, Pintar JE, Zheng J, Friedman WF, Zhou X, Zaremba T. 2000. Autocrine expression and ontogenetic functions of the PACAP ligand/receptor system during sympathetic development. Dev Biol 219:197–213.

Dijkstra CD, Dopp EA, Joling P, Kraal G. 1985. The heterogeneity of mononuclear phagocytes in lymphoid organs: distinct macrophage subpopulations in the rat recognized by monoclonal antibodies ED1, ED2 and ED3. Immunology 54:589–599.

Dornay M, Gilad VH, Shiler I, Gilad GM. 1986. Early polyamine treatment accelerates regeneration of rat sympathetic nerouns. Exp Neurol 92:665–674.

Elfvin LG, Bjorklund H, Dahl D, Seiger A. 1987. Neurofilament-like and glial fibrillary acidic protein-like immunoreactivities in rat and guinea pig sympathetic ganglia in situ and after perturbation. Cell Tissue Res 250:79–86.

Esch F, Lin KI, Hills A, Zaman K, Baraban JM, Chatterjee S, Rubin L, Ash DE, Ratan RR. 1998. Purification of a multipotent antideath activity from bovine liver and its identification as arginase: nitric oxide-independent inhibition of neuronal apoptosis. J Neurosci 18:4083–4095.

Festoff BW, Nelson PG, Brenneman DE. 1996. Prevention of activity-dependent neuronal death: vasoactive intestinal polypeptide stimulates astrocytes to secrete the thrombin-inhibiting neurotrophic serpin, protease nexin I. J Neurobiol 30:255–266.

Figiel M, Engele J. 2000. Pituitary adenylate cyclase-activating polypeptide PACAP, a neuron-derived peptide regulating glial glutamate transport and metabolism. J Neurosci 20:3596–3605.

Funk JL, Trout CR, Wei H, Stafford G, Reichlin S. 2001. Parathyroid hormone-related protein PTHrP induction in reactive astrocytes following brain injury: a possible mediator of CNS inflammation. Brain Res 915:195–209.

Gilad GM, Gilad VH. 1983. Early rapid and transient increase in ornithine decarboxylase

activity within sympathetic neurons after axonal injury. Exp Neurol 81:158–166.

Gilad VH, Tetzlaff WG, Rabey JM, Gilad GM. 1996. Accelerated recovery following polyamines and aminoguanidine treatment after facial nerve injury in rats. Brain Res 724:141–144.

Giralt M, Penkowa M, Lago N, Molinero A, Hidalgo J. 2002. Metallothionein-1+2 protect the CNS after a focal brain injury. Exp Neurol 173:114–128.

Gorman AM, McGowan A, O'Neill C, Cotter T. 1996. Oxidative stress and apoptosis in neurodegeneration. J Neurol Sci Suppl 139:45–52.

Holmes FE, Mahoney S, King VR, Bacon A, Kerr NCH, Pachnis V, Curtis R, Priestley JV, Wynick D. 2000. Targeted disruption of the galanin gene reduces the number of sensory neurons and their regenerative capacity. Proc Natl Acad Sci USA 97:11563–11568.

Hyatt-Sachs H, Schreiber RC, Bennett TA, Zigmond RE. 1993. Phenotypic plasticity in adult sympathetic ganglia in vivo: effects of deafferentation and axotomy on the expression of vasoactive intestinal peptide. J Neurosci 13:1642–1653.

Jander S, Bussini S, Neuen-Jacob E, Bosse F, Menge T, Muller HW, Stoll G. 2002. Osteopontin: a novel axon-regulated Schwann cell gene. J Neurosci Res 67:156–166.

Jean JC, Oakes SM, Joyce-Brady M. 1999. The Bax inhibitor-1 gene is differentially regulated in adult testis and developing lung by two alternative TAT-less promoters. Genomics 57:201–208.

Kato R, Kiryu-Seo S, Kiyama H. 2002. Damage-induced neuronal endopeptidase DINE/ECEL expression is regulated by leukemia inhibitory factor and deprivation of nerve growth factor in rat sensory ganglia after nerve injury. J Neurosci 22:9410–9418.

Kepka-Lenhart D, Mistry SK, Wu G, Morris SM Jr. 2000. Arginase I: a limiting factor for nitric oxide and polyamine synthesis by activate macrophages? Am J Physiol 279:R2237–R2242.

Kiryu-Seo S, Sasaki M, Yokohama H, Nakagomi S, Hirayama T, Aoki S, Wada K, Kiyama H. 2000. Damage-induced neuronal endopeptidase DINE is a unique metallopeptidase expressed in response to neuronal damage and activates superoxide scavengers. Proc Natl Acad Sci USA 97:4345–4350.

Koo EH, Hoffman PN, Price D. 1988. Levels of neurotransmitter and cytoskeletal protein mRNAs during nerve regeneration in sympathetic ganglia. Brain Res 449:361–363.

Li H, Meininger CJ, Kelly KA, Hawker JR Jr, Morris SM Jr, Wu G. 2002. Activities of arginase I and II are limiting for endothelial cell proliferation. Am J Physiol 282:R64–R69.

Livesey FJ, O'Brien JA, Li M, Smith AG, Murphy LJ, Hunt SP. 1997. A Schwann cell mitogen accompanying regeneration of motor neurons. Nature 390:614–618.

Magnusson S, Ekstrom TJ, Elmer E, Kanje M, Ny L, Alm P. 2000. Heme oxygenase-1, heme oxygenase-2 and

biliverdin reductase in peripheral ganglia from rat; expression and plasticity. Neuroscience 95:821–829.

Magnusson S, Kanje M. 1998. Differential macrophage responses following pre- and postganglionic axotomy. Neuroreport 9:841–846.

Mahoney SA, Hosking R, Farrant S, Holmes FE, Jacoby AS, Shine J, Iismaa TP, Scott MK, Schmidt R, Wynick D. 2003. The second galanin receptor GALR2 plays a key role in neurite outgrowth from adult sensory neurons. J Neurosci 23:416–421.

Manni L, Aloe L, Tirassa P, Finn A, Lundeberg T. 2001. Cholecystokinin-8 promotes recovery of sympathectomy induced by 6-hydroxydopamine in adult mice. Neuroreport 12:1621–1627.

Martinez C, Delgado M, Pozo D, Leceta J, Calvo JR, Ganea D, Gomariz RP. 1998. VIP and PACAP enhance IL-6 release and mRNA levels in resting peritoneal macrophages: in vitro and in vivo studies. J Neuroimmunol 85:155–167.

Matthews MR, Raisman G. 1972. A light and electron microscopic study of the cellular response to axonal injury in the superior cervical ganglion of the rat. Proc R Soc Lond B Biol Sci 181:43–79.

Mohney RP, Siegel RE, Zigmond RE. 1994. Galanin and vasoactive intestinal peptide messenger RNAs increase following axotomy of adult sympathetic neurons. J Neurobiol 25:108–118.

Moller K, Reimer M, Ekblad E, Hannibal J, Fahrenkrug J, Kanje M, Sundler F. 1997. The effects of axotomy and preganglionic denervation on the expression of pituitary adenylate cyclase activating peptide (PACAP), galanin and PACAP type 1 receptors in the rat superior cervical ganglion. Brain Res 775:166–182.

Monard D. 1993. Tinkering with certain blood components can engender distinct functions in the nervous system. Perspect Dev Neurobiol 1:165–168.

Mori T, Iijima N, Kitabatake K, Kohsaka S. 1990. Alpha 2-macroglobulin is an astroglia-derived neurite-promoting factor for cultured neurons from rat central nervous system. Brain Res 527:55–61.

Nagarajan R, Le N, Mahoney H, Araki T, Milbrandt J. 2002. Deciphering peripheral nerve myelination by using Schwann cell expression profiling. Proc Natl Acad Sci USA 99:8998–9003.

O'Quinn PR, Knabe DA, Wu G. 2002. Arginine catabolism in lactating porcine mammary tissue. J Anim Sci 80:467–474.

Purves D. 1975. Functional and structural changes in mammalian sympathetic neurones following interruption of their axons. J Physiol 252:429–463.

Rao MS, Sun Y, Escary JL, Perreau J, Tresser S, Patterson PH, Zigmond RE, Brulet P, Landis SC. 1993a. Leukemia inhibitory factor mediates an injury response but not a target-directed developmental switch in sympathetic neurons. Neuron 11:1175–1185.

Rao MS, Sun Y, Vaidyanathan U, Landis SC, Zigmond RE. 1993b. Regulation of substance P is similar to that of vasoactive intestinal peptide after axotomy or explantation of the rat superior cervical ganglion. J Neurobiol 24:571–580.

Sato T, Ito A, Mori Y. 1990. Interleukin 6 enhances the production of tissue inhibitor of metalloproteinases (TIMP) but not that of matrix metalloproteinases by human fibroblasts. Biochem Biophys Res Commun 170: 824–829.

Schafer H, Trauzold A, Siegel EG, Folsch UR, Schmidt WE. 1996. PRG1: a novel early-response gene transcriptionally induced by pituitary adenylate cyclase activating polypeptide in a pancreatic carcinoma cell line. Cancer Res 56:2641–2648.

Schreiber RC, Hyatt-Sachs H, Bennett TA, Zigmond RE. 1994. Galanin expression increases in adult rat sympathetic neurons after axotomy. Neuroscience 60:17–27.

Schreiber RC, Shadiack AM, Bennett TA, Sedwick CE, Zigmond RE. 1996. Changes in the macrophage population of the rat superior cervical ganglion after postganglionic nerve injury. J Neurobiol 27:141–153.

Schreiber RC, Vaccariello SA, Boeshore K, Shadiack AM, Zigmond RE. 2002. A comparison of the changes in the non-neuronal cell populations of the superior cervical ganglia following decentralization and axotomy. J Neurobiol 53:68–79.

Seiler N. 2000. Oxidation of polyamines and brain injury. Neurochem Res 25:471–490.

Shewan D, Calaora V, Nielsen P, Cohen J, Rougon G, Moreau H. 1996. mCD24, a glycoprotein transiently expressed by neurons, is an inhibitor of neurite outgrowth. J Neurosci 16:2624–2634.

Smith DS, Skene JH. 1997. A transcription-dependent switch controls competence of adult neurons for distinct modes of axon growth. J Neurosci 17:646–658.

Sun Y, Rao MS, Zigmond RE, Landis SC. 1994. Regulation of vasoactive intestinal peptide expression in sympathetic neurons in culture and after axotomy: the role of cholinergic differentiation factor/leukemia inhibitory factor. J Neurobiol 25:415–430.

Sun Y, Zigmond RE. 1996a. Involvement of leukemia inhibitory factor in the increases in galanin and vasoacitve intestinal peptide mRNA and the decreases in neuropeptide Y and tyrosine hydroxylase mRNA in sympathetic neurons after axotomy. J Neurochem 67:1751–1760.

Sun Y, Zigmond RE. 1996b. Leukemia inhibitory factor induced in the sciatic nerve after axotomy is involved in the induction of galanin in sensory neurons. Eur J Neurosci 8:2213–2220.

Tanaka S, Koike T. 1994. Vasoactive intestinal peptide suppresses neuronal cell death induced by nerve growth factor deprivation in rat sympathetic ganglion cells in vitro. Neuropeptides 26:103–111.

Thompson SWN, Priestley JV, Southall A. 1998. GP130 cytokines, leukemia inhibitory factor and interleukin 6, induce neuropeptide expression in intact adult rat sensory neurons in vivo: time-course, specificity and comparison with sciatic nerve axotomy. Neuroscience 84:1247–1255.

Tsujino H, Kondo E, Fukuoka T, Dai Y, Tokunaga A, Miki K, Yonenobu K, Ochi T, Noguchi K. 2000. Activating transcription factor 3 ATF3. induction by axotomy in sensory and motoneurons: a novel neuronal marker of nerve injury. Mol Cell Neurosci 15:170–182.

Wang H, Sun H, Della Penna K, Benz RJ, Xu J, Gerhold D,

Holder DJ, Koblan KS. 2002. Chronic neuropathic pain is accompanied by global changes in gene expression and shares pathobiology with neurodegenerative diseases. Neuroscience 114:529–546.

Waschek JA. 2002. Multiple actions of pituitary adenylyl cyclase activating peptide in nervous system development and regeneration. Dev Neurosci 24:14–23.

Watson WE. 1974. Cellular responses to axotomy and to related procedures. Br Med Bull 30:112–115.

Zhang QL, Lin PX, Shi D, Xian H, Webster HD. 1996. Vasoactive intestinal peptide: mediator of laminin synthesis in cultured Schwann cells. J Neurosci Res 43:496–502.

Zhang X, Dagerlind A, Bao L, Ji RR, Lundberg JM, Hokfelt T. 1994. Increased expression of galanin in the rat superior cervical ganglion after pre- and postganglionic nerve lesions. Exp Neurol 127:9–22.

Zigmond RE, Hyatt-Sachs H, Mohney RP, Schreiber RC, Shadiack AM, Sun Y, Vaccariello SA. 1996. Changes in neuropeptide phenotype after axotomy of adult peripheral neurons and the role of leukemia inhibitory factor. Perspect Dev Neurobiol 4:75–90.

Zurn AD, Nick H, Monard D. 1988. A glia-derived nexin promotes neurite outgrowth in cultured chick sympathetic neurons. Dev Neurosci 19:17–24.